

# Resistivity Structure of the North West Olkaria Field Using 1D Inversion of Magnetotelluric Data

Sirma Chebet Ruth<sup>1</sup>, Msk. Kirui<sup>2</sup>, Nicholas Mariita<sup>3</sup>, Wafula Chembeni Peter<sup>4</sup>

<sup>1,2,4</sup>Department of Physics, Egerton University Njoro campus, P.O. Box 536 - 20155, Egerton

<sup>2</sup>Dedan Kimathi University, Private Bag Nyeri, Kenya

**Abstract:** The Northwest Olkaria prospect is part of the Greater Olkaria Geothermal Area located within the Kenyan rift in Nakuru County. It is bounded by the longitudes  $36^{\circ} 15' E'$  and  $36^{\circ} 12' E'$  with an estimated area of  $30 \text{ Km}^2$ . The area has been the least studied sector of the Greater Olkaria Geothermal Area due to its remote location and complex terrain. The study used the Magnetotelluric method to determine the electrical resistivity distribution of the subsurface and locate structural features controlling the geothermal distribution in the prospect area. A total of 52 Magnetotelluric soundings were considered in this research project and 47 corresponding central loop Transient Electromagnetic soundings. To allow the static shift correction in the 1D inversion, the Magnetotelluric data were jointly inverted with Transient Electromagnetic data. The results and interpretations of the Joint 1D inversion of Magnetotelluric and central loop Transient Electromagnetic data of Olkaria Northwest prospect were presented in form of resistivity Iso-maps and cross sections. These inversions were achieved by fitting both data kinds using the same 1D resistivity model. The result of the interpretation shows three main resistivity structures below the prospect area: (1) A shallow superficial lying thin high resistivity layer ( $> 30 \Omega\text{m}$ ) thought to be due to unaltered rock formations and the thick pyroclastic cover is observed across the prospect followed by low resistivity thick dome shaped conductive layer ( $< 6 \Omega\text{m}$ ) that extends to about 200 m.a.s.l in the North West field and thins towards the Central field becoming almost uniform in the South East and the rest of the field. This layer is presumed to be dominated by low temperature alteration minerals such as smectite and zeolite that defines the clay cap. (2) A high resistivity layer (resistive core) underlain by a deep lying conductor ( $> 15-50 \Omega\text{m}$ ) which is thought to be associated with the high temperature secondary minerals such as epidote, chlorite and biotite that are present in the reservoir. (3) A low conductivity layer that extends to about 6,000 m.b.s.l. which is associated with the heat source. Among the many recommendations highlighted, the study revealed that the main reservoir to the western side appears to be deeper than the known situation in the eastern field, at great depths, a prominent low resistive cap is observed and it is probably reflecting the presence of heat source of the geothermal system underneath the Northwest Olkaria prospect.

**Keywords:** Northwest Olkaria, Magnetotelluric, Transient Electromagnetic, Resistivity, 1D Inversion, static shift

## 1. Introduction

Olkaria Geothermal field is a high temperature geothermal resource in the Kenyan Rift Valley which has been used for electricity generation since 1981 (Omenda and Simiyu, 2015). Olkaria geothermal area has been divided into seven development sectors out of which only three have been committed to development. The fields are Olkaria East, Olkaria Northeast, Olkaria South West, Olkaria Central, Olkaria North West, Olkaria South East and Olkaria Domes. The fields are named with respect to Olkaria Hill (Omenda, 2000; Ouma, 2010). The Northwest Olkaria prospect is part of the Greater Olkaria Geothermal Area located within the Kenyan rift in Nakuru County. It is bounded by the longitudes  $36^{\circ} 15' E'$  and  $36^{\circ} 12' E'$  with an estimated area of  $30 \text{ Km}^2$  (Omenda, 2000; Ouma, 2010). The area has been the least studied sector of the Greater Olkaria Geothermal Area due to its remote location and complex terrain.

## 2. Geological and Tectonic Setting

The Great Africa Rift System (GARS) which is a major tectonic structure stretches to about 6100 km from the Red Sea in the north to Mozambique in the south (Shako and Wamalwa, 2014). The rift starts from a triple junction which is evident in Ethiopia, at this point two branches are in contact with the Red Sea and the Gulf of Eden and the third is towards the south passing through Ethiopia (Omenda and Simiyu, 2000). Olkaria Geothermal Complex is located in one of the eastern arms of the GARS stretching through

Eritrea, Ethiopia, and Kenya and all the way down to Mozambique (Figure 1).



**Figure 1:** Structural map showing the East African Rift System (Omenda and Simiyu, 2000).

The Great Africa Rift system was formed in more or less a linear like zone where the continental plate is being pulled apart with the rifting between widened mantle plume that probably began under east Africa, creating three arms; East Africa Rift, Gulf of Eden Rift and Red Sea Rift (Omenda, 1994). The heat flow from the asthenosphere along the rift zones lead to volcanism and the formation of the domes as can be seen in Olkaria. The eastern branch is believed to be much older and considered to have developed about 13 to 23 million years earlier before the western branch and this was supported by the discovery of preserved vertebrate fossils and volcanic ash which are believed to be about 23 million years old (Ring, 2014).

The rifting activity in the Kenya Rift began about 30 million years ago with uplift in the Lake Turkana area and then

migrated southward being more intense about 14 million years ago. Formation of the graben structure in Kenya started about 5 million years ago and was followed by fissure eruptions in the axis of the rift to form flood lavas by about 2 to 1 million years ago. During the last 2 million years ago, volcanic activities became more intense within the axis of the rift due to extension. (Girdler, 2013; Mulwa and Mariita, 2013, 2015; Wamalwa *et al.*, 2013; Wamalwa and Serpa, 2013; Abdelfettah *et al.*, 2016). During this time, large shield volcanoes, most of which are geothermal prospects, developed in the axis of the rift. The volcanoes include Suswa, Longonot, Olkaria, Eburru, Menengai, Korosi, Paka, Silali, Emuruangogolak and Barrier.

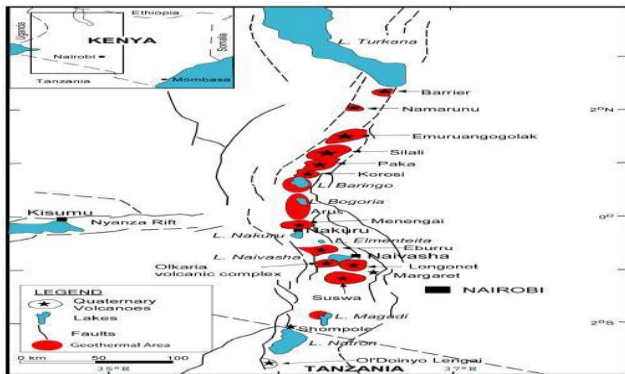


**Figure 2:** Map showing the location of the Greater Olkaria Geothermal Area within the Great Rift Valley of Kenya. (Ofwona, 2008)

### 3. Geology of Olkaria Geothermal Area

Figure 2 shows the rift structure in Kenya along with the distribution of central volcanic complexes in the Eastern African Rift structure (Renaut *et al.*, 2017). Olkaria central volcanic complex is positioned in the part of the rift system where it changes from near north direction to a north-westerly one. Olkaria similarly has a north-westerly elongation with Longonot volcano aligned in a similar way ESE of Olkaria. This arrangement indicates both NW-SE and N-S structural trends. (KenGen, 2014)

Olkaria has a more complex volcanic build-up. West-JEC (2009) states that although major fractures and faults are observed on surface, their offset and throws are difficult to ascertain due to their limited exposures and loose unconsolidated surface cover and vegetation. The main tectonic structures are aligned N-S and NW-SE, WNW-ESE and NE-SW (Omenda, 2000). The second type of tectonic structures is the ring structures. They are most notable in the south and southeast, but less clear in other areas. It is, however, interesting to see the various interpretations of ring structures. As the focus in the current study is on the NW area, it is interesting to note that the proposed ring structure is split into an inner and outer ring in the southeast. In the literature these structures are either named calderas or ring structures, where the former indicates the formation of a cauldron, while the latter may not. Apparently, evidence for a cauldron filled up with eruptive material, has not been conclusively identified (Renaut *et al.*, 2017). It is interesting, however, to compare Olkaria with other caldera structures in neighboring volcanic complexes, like Menengai, where multiple caldera structures of variable circumferences are

evident (Omenda, 2000; Ouma, 2010; Omenda and Simiyu, 2015). Even Longonot, east of Olkaria appears to have several radial features, and one may be tempted to argue the same for Olkaria. The meaning of that implies more fracture patterns, which affects and adds to the permeability related structures of the reservoir.

Exposed volcanic formations consist of rhyolitic lavas and pyroclastic rocks, the latter mainly derived from the neighboring Longonot volcano. The eruptions of rhyolite lavas and domes are strongly related to five N-S tectonic structures, four of which cross the Olkaria ring structure (Ofwona, 2008). They, furthermore, appear to erupt along the ring structures as is particularly evident in the east and south. Further to that is a WNW-ESE structure that passes through the centre of the ring structure and where it crosses the N-S eruption structures, a larger rhyolite effusion is apparently seen. The overall volume of eruptives appears to be small but extensively distributed along the ring structures and tectonic fractures (Wamalwa and Serpa, 2013). The youngest rhyolite, OlButot rhyolite, in Olkaria is dated at about 200 years. Ring or caldera structures are clearly related to magmatic activity, as is evident by the close association of these with magma extrusion (Wadheet *et al.*, 2016) Whether the feeders of the rhyolites ascent up vertical "caldera" faults, or if they might be in the form of cone sheets, has not been discussed, but appears to be taken as of the former type (Prodehl *et al.*, 1997).

The volcanic activity may relate to the geothermal one in several ways. It may firstly ascend up from the magma heat source into the geothermal system, up into the cold groundwater system and to surface. The volcanic feeders may secondly be short-lived localized heat sources where the magma consolidates and assimilates its heat to the surrounding rock mass (Odera, 2016). It may thirdly form permeable structures for geothermal flow as well as forming barriers to flow oblique to the structure (this condition may though deteriorate with age and later superimposed tectonic activity). The common occurrence of geothermal manifestations along the permeable structures, are clear indications of the ascent of geothermal fluids, at least from the upper part of the system to surface (Abdelfettah *et al.*, 2016).

### 4. Magnetotelluric Physics

The MT method is an electromagnetic (EM) sounding technique that uses surface measurements of the natural electric (E) and magnetic (B) fields to infer the subsurface electrical resistivity distribution. This method relies on the detection of small potential differences generated by electromagnetic waves propagated from the ionosphere (Ward and Wannamaker, 1983). The natural source of MT fields originates from lightning discharges and magnetospheric current systems set up by solar activity. These sources create a spectrum of EM fields in the frequency band  $10^{-4}$  Hz to  $10^4$  Hz that provide information used to delineate structures at depth, from a few tens of meters to the upper mantle (a few tens of kilometers). MT data at various frequencies provide a means to distinguish spatial variations in resistivity vertically and laterally. The EM field penetration, which decays exponentially, is related

to the frequency and resistivity of the medium. Higher frequencies map the near-surface resistivity distribution. Lower frequencies that penetrate deeper provide information on deeper structures. (Christiansen *et al.*, 2006). The apparent resistivity for decreasing frequencies thus provides resistivity information at progressively increasing depths and is essentially a form of vertical electrical sounding. Near surface resistivity in homogeneities has been found to distort the electric field since the field is discontinuous across a resistivity boundary. This distortion is known as static shift. This effect shifts the MT sounding curve (of apparent resistivity versus period) by some constant scale factor. Since the magnetic field is relatively unaffected by static shift, a controlled source magnetic field sounding such as TEM can be used to correct for static shift. The MT sounding curve is shifted vertically so that the high frequency part of the MT curve coincides with the TEM curve. The low frequency MT curve then gives an undistorted view of the deep resistivity section (Jones, 1988). To understand the Magnetotelluric method, consider a plane EM wave that is incident on the surface of the Earth. The resistivity of the Earth is much lower than the atmosphere, thus an EM signal travels as a wave in the air and diffuses in the Earth. The fundamental differential equations governing the behavior of electromagnetic fields are given by Maxwell's equations

$$\nabla \cdot \mathbf{E} = \frac{\rho}{\epsilon} \quad (1)$$

$$\nabla \cdot \mathbf{B} = 0 \quad (2)$$

$$\nabla \times \mathbf{H} = \sigma \mathbf{E} + \epsilon \frac{\partial \mathbf{E}}{\partial t} \quad (3)$$

$$\nabla \times \mathbf{E} = -\frac{\partial \mathbf{B}}{\partial t} \quad (4)$$

Where  $\mathbf{E}$  is the electric field strength in  $V/m$ ,  $\mathbf{H}$  is the magnetic field strength,  $\mathbf{B}$  is the magnetic flux density  $W/m^2$ ,  $\rho$  is the volume charge density in  $C/m^3$ ,  $\sigma$  is the conductivity in  $S/m$ ,  $\epsilon$  is the dielectric constant in  $F/m$ . Where  $\mathbf{J} = \sigma \mathbf{E}$  and  $\mathbf{B} = \mu \mathbf{H}$ , equation 4 can be rewritten as equation 5

$$\nabla \times \mathbf{B} = \mu \mathbf{J} + \mu \epsilon \frac{\partial \mathbf{E}}{\partial t} \quad (5)$$

Here  $\mathbf{J}$  is the current density in  $A/m^2$ , and  $\mu$  is magnetic permeability in  $H/m$ . Usually the free space values  $\mu_0 = 4\pi \times 10^{-7} H/m$  and  $\epsilon_0 = 8.85 \times 10^{-12} F/m$  are used in these equations.

Taking the curl of equation 4 and using equation 5, a second order partial differential equation for  $\mathbf{E}$  alone can be obtained

$$\nabla^2 \mathbf{E} = \mu \sigma \frac{\partial \mathbf{E}}{\partial t} + \mu \epsilon \frac{\partial^2 \mathbf{E}}{\partial t^2} \quad (6)$$

In the case of a dielectric environment, there is minimal conduction current, and the displacement current dominates. Thus equation 7 can be simplified to the wave equation:

$$\nabla^2 \mathbf{E} - \mu \epsilon \frac{\partial^2 \mathbf{E}}{\partial t^2} = 0 \quad (7)$$

In the case of a conductive environment, the conduction current dominates and the effect of displacement current can be ignored. Thus equation 8 can be simplified to the diffusion equation:

$$\nabla^2 \mathbf{E} - \mu \sigma \frac{\partial \mathbf{E}}{\partial t} = 0 \quad (8)$$

The Earth can be treated as the conductive environment, so the diffusion equation can be used in MT data analysis. For

an EM wave with a sinusoidal time variation, the electric field strength can be written as:

$$\nabla^2 \mathbf{E} + i\omega \mu \sigma \mathbf{E} = 0 \quad (9)$$

Note that due to the transformation of electromagnetic energy into heat, the strength of the fields decreases exponentially with depth. Consider a wave that travels in the Earth with exponential amplitude decay in the  $z$  direction, equation 9 can be written as:

$$\frac{\partial^2 \mathbf{E}}{\partial z^2} + i\omega \mu \sigma \mathbf{E} = 0 \quad (10)$$

Where  $E_0$  is the electric field strength at the Earth's surface, equation 10 can be written as:

$$E k^2 + i\omega \mu \sigma E = 0 \quad (11)$$

Rearranging this formula gives:

$$E(k^2 + i\omega \mu \sigma) = 0 \quad (12)$$

Then solving for  $k$ :

$$k = \pm(1 - i) \sqrt{\frac{i\omega \mu \sigma}{2}} \quad (13)$$

Here  $k$  is the complex wave number of the medium;  $E_s$  is the horizontal electric field at the surface. So the field propagate in Earth can be written as:

$$E_s = E_0 e^{i\omega t} e^{i\sqrt{\frac{i\omega \mu \sigma}{2}} z} e^{-\sqrt{\frac{i\omega \mu \sigma}{2}} z} \quad (14)$$

In equation 18, the exponential term represents the decay of the amplitude as wave travels in the  $z$  direction. Skin depth is defined as the distance ( $\delta$ ) over which the electric field strength is attenuated by  $\frac{1}{e}$  of the original field strength. Since

$$e^{-\sqrt{\frac{i\omega \mu \sigma}{2}} \delta} = e^{-1} \quad (15)$$

The skin depth can be written as:

$$\delta = \sqrt{\frac{2}{\omega \mu \sigma}} \quad (16)$$

Equation 16, it can be shown that:

$$\delta \approx 503 \sqrt{\frac{\rho}{f}} (m) \quad (17)$$

## 5. Processing of Magnetotelluric Data

Time-series data was downloaded using the SSMT2000 program from the MT unit and were processed using MT Editor provided by Phoenix Geophysics-Canada. The SSMT2000 was used for configuring MT instrumentation and parameters. The MT Editor Programme accepted MT plots output by SSMT2000, merged the cross powers and displayed MT parameters graphically (Boashash, 2015). It also enabled elimination of cross powers from the calculations and hence the possibility of editing out poor quality data. The primary objective of editing was to create a smooth resistivity curve by eliminating those cross powers that had moved too far from the mean by noise and related effects. Though it was possible to eliminate data points from being considered, the software did not delete them completely. It placed a mask on those unwanted cross powers, allowing reversion to the original data at any time.



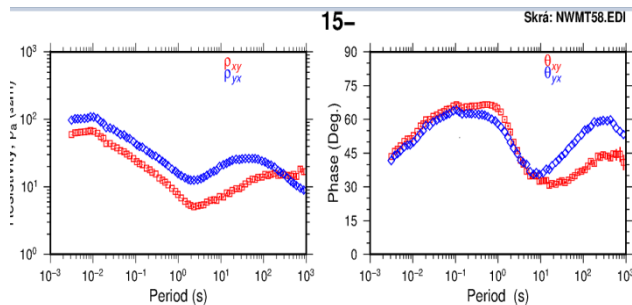


**Figure 3:** Processed MT apparent resistivity and phase curves of an MT sounding in the NW Olkaria field ( $\rho_{xy}$  and  $\Theta_{xy}$ ; TE mode is in red while  $\rho_{yx}$  and  $\Theta_{yx}$  TM mode are in blue) (NWMT58.EDI).

Figure 3 shows that there is a 1D response with decreasing resistivity for periods below 1s. The final cross-powers and auto-powers, as well as all relevant MT parameters calculated, were stored in EDI files which are the industry's standard. These EDI files were then used as input for the Linux program TEMTD where they were used for joint inversion with TEM (Boashash, 2015). A well-established method for static shift correction of MT data was then used with TEM (Stenberg *et al.*, 1988; Pellerin and Hohmann, 1990). The imported 1-D model was used to calculate a forward MT response. The observed apparent resistivity curve was then shifted along the resistivity axis to coincide with the values suggested by the TEM response (Khazri and Gabtni, 2018).

## 6. Joint Inversion of TEM and MT Data

A number of cross sections were made to display the result of the 1D inversion of the MT and TEM soundings. The programme Temtd performed 1D Inversion with horizontally layered earth models of central-loop Transient Electro-Magnetic and Magnetotelluric data. It was used to invert only TEM or MT data and also for joint inversion of TEM and MT data, in which case it determined the best static shift parameter for the MT data. For TEM data, the programme assumed that the source loop was a square loop and that the receiver coil/loop was at the center of the source loop. The current wave form was assumed to be half-duty bipolar semi-square wave (equal current-on and current-off segments), with exponential current turn-on and linear current turn-off. For MT data, the programme assumed standard EDI for of impedance and/or apparent resistivity and phase data. The programme is written in ANSI-C and runs under UNIX/LINUX operating systems. It uses the g.n.u plot graphics programme for graphical display during the inversion process (Árnason, 2006). Joint inversion of MT and TEM data was performed to deduce 1D smooth models of the subsurface resistivity structure as well as resistivity isomaps at different depths, elevations and periods/frequencies. Layered resistivity models were then calculated from the smooth models.

## 7. Results and Discussions

These results present the geophysical work performed in Olkaria Northwest in the Greater Olkaria Geothermal Area which covered Magnetotelluric and Transient Electromagnetic surveys. The surveys involved data

acquisition, processing and interpretation using a one dimensional joint inversion of the data sets based on a nonlinear least-squares inversion of the Levenberg-Marquardtcode, (Árnason, 1989) and the results are presented both by iso-resistivity maps at different elevations and resistivity cross-sections along selected profiles. The EM data that were used in this project were collected from 21<sup>st</sup> September to 19<sup>th</sup> November 2015 where 52 MT soundings and 47 TEM soundings were collected for deeper lying structures. The joint processing technique was used to correct the static shift problems encountered by MT.

The aim of this study was to establish the resistivity structure of this field and to correlate it with the alteration mineralogy and the geological well data from a few wells that have been drilled in this field in the past. An attempt was also made to suggest possible locations for future drill holes by considering the outcome of the correlations above and hence determine the geothermal potential of the survey area.

In this study a total of 47 TEM (Figure 4) and 52 MT soundings spread over an area of about 30km<sup>2</sup> were carried out in Olkaria North West using the central loop TEM configuration which involved transmission of a half-duty (50% duty circle) square wave current into a transmitter loop at frequencies of 16Hz and 4Hz using Zonge TEM system from Zonge Engineering (USA) that is comprised of a transmitter, 24 bit multifunction receiver, voltage regulator, 1.0mm<sup>2</sup> transmitter cable and a receiver coil with a dipole moment of about 10000Am<sup>2</sup>. In the field setup, depending on the available space either a 300 x 300 or a 200 x 200 transmitter loop was used to transmit the half duty current wave at the frequencies stated above. In both cases the transient signal was recorded at the center of the loop at time intervals with logarithmically spaced- sampling time gates after the current turn-off.

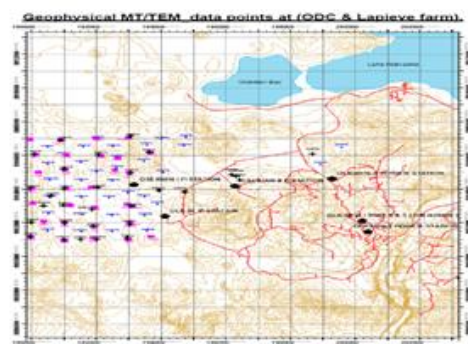


**Figure 4:** Map showing done TEM and MT points

### 7.1 1D Cross-sections

Resistivity cross-sections are plotted for results obtained from 1D inversion by petrel program, developed by Slumberger (<https://www.software.slb.com/products/petrel>). The programme calculates the best line between selected soundings on a profile, and plots resistivity iso-lines based on the 1D model for each sounding. It is actually the logarithm of the resistivity that is contoured so the colour scale is exponential but numbers at contour lines are actual resistivity values. Several cross-sections were made through

the survey area and profiles were positioned perpendicular to the inferred geoelectrical strike.

### 7.2 NS moving WE direction

These profiles trend in the NS direction and show the variation of conductivity from West to East at different depths above sea level (figure 5). The resistivity structure generally shows a four-layer high-low-high-low resistivity trend. The topmost >30 ohm-m resistivity layer coincides with the unaltered formation and the superficial deposit on the surface. Beneath this thin high resistivity layer is a thick layer of a very conductive >6 ohm-m dome-like layer that extends up to 200 m.a.s.l coinciding to low to medium temperature alteration and is interpreted as the clay cap. It is a zone that is dominated by conductive alteration minerals such as smectites and zeolites. Beneath the base of this conductor is a resistive >15-50 ohm-m which is associated with the high temperature secondary minerals such as epidote, chlorite and biotite present in the reservoir. Beneath the resistive layer is another low conductivity layer extending to about 6,000 M.b.s.l and it is associated with the heat source.

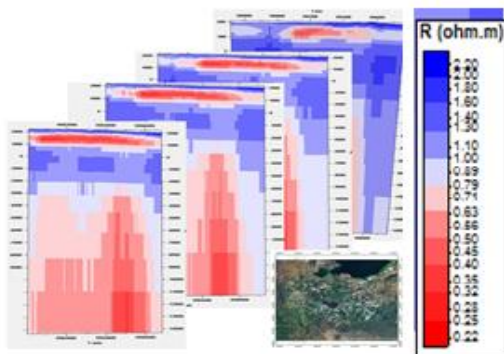


**Figure 5:** Profiles trend in the NS direction and shows the variation of conductivity from West to East at different depths above sea level

The cross-sections are dissecting the area in N-S direction (Figure 6) across the production field of Olkaria. The resistivity structure generally shows a four-layer high-low-high-low resistivity trend. There is a very good agreement between the resistive anomalies and the most productive wells. The deep wells in domes and Olkaria Central field correspond to the deep high resistivity anomaly defined by MT data, while the low productive wells fall within the generally conductive shallow subsurface layer.

The shallow structure reflects the lithological response of shallow formations, which are quite conductive interpreted to due to the presence of low temperature alteration minerals. It is clear that the low resistivity cap on the western side is of different with the low resistivity on the Eastern side.

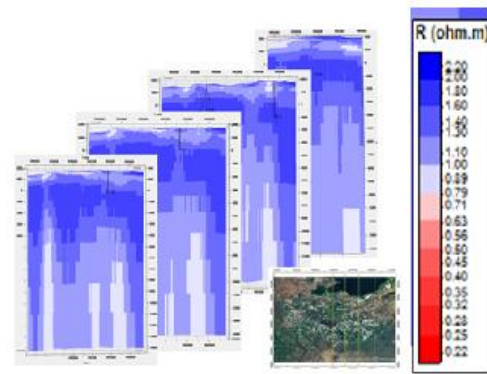


**Figure 6:** Cross-Section N-S direction at 6000 m.b.s.l

The western side is too conductive and thicker than the eastern side. Lack of alteration mineralogy of the drilled wells to the West (Oserian Wells) has made it difficult to correlate the alteration mineralogy with resistivity. The alteration mineralogy on the Eastern part of the study area is in agreement with resistivity. However, where geological information is available and the geometry of the formations is known, the two different effects can be separated.

### 7.3 W-E Cross-Section (East -West moving from North-South)

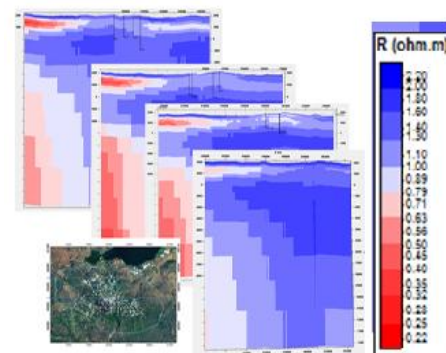


**Figure 7:** Profiles running W-E at 6000 m.b.s.l

The above profiles presented in figure 7 are running W-E direction covering about 20 km. The resistivity structure generally shows a four-layer high-low-high-low resistivity trend. The high resistivity near surface is uniform along the profile and is associated with the presence of unaltered formations and superficial deposits. This is underlain by a low resistivity which is not uniform along the profile. The western side possesses a highly conductive and probably much more conductive than the Illitic clays and other high temperature mineralization that occur above 200°C. Therefore, in most high temperature geothermal systems, there is a characteristic clay “cap” that forms above the main high temperature reservoir and often on the sides of geothermal systems, particularly in outflow areas. This clay cap is readily the most dominant feature seen by resistivity surveys and so provides a useful indicator of the location and extent of the underlying higher temperature reservoir. The clay cap layer to the western side is thicker than the clay cap to the eastern side which might lead to change in the casing design and depth of drilling to accommodate the high temperature zone. The base of the clay cap usually marks the transition to high temperature reservoir (or, at least, reservoir



at temperature greater than 200°C) and can be treated as a thermal indicator. The top of the cap typically marks the upper extent of thermal activity (about 50°C). Underlying the clay cap is resistive layer interpreted to be due to the presence of high temperature alteration and believed to be the main reservoir. This layer is very thin to eastern side and appear to be deep but the same layer is very thick along the profile to the east and very deep which might mean the reservoir to eastern side is thin and very deep. The conductive layer below the main reservoir system can be interpreted to be due to the presence of heat source.

#### 7.4 1D Iso-Resistivity Maps

Iso-resistivity maps are made by a program known as TEMRESD which generates iso-resistivity maps at fixed elevations derived from the 1D Occam models (Eysteinnsson, 1998). The resistivity is contoured and coloured in algorithmic scale. The general elevation of the area in m.a.s.l. In the following section Iso-resistivity maps are presented from 2000 m.a.s.l. down to 6000 M.b.s.l. The maps show that resistivity varies considerably both laterally and with depth.

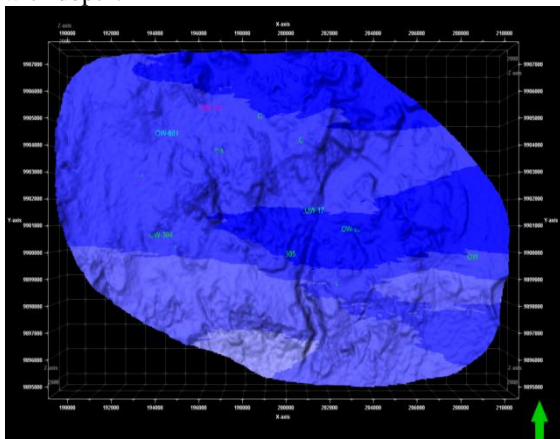


Figure 8: Iso-Resistivity map at 2000 m.a.s.l

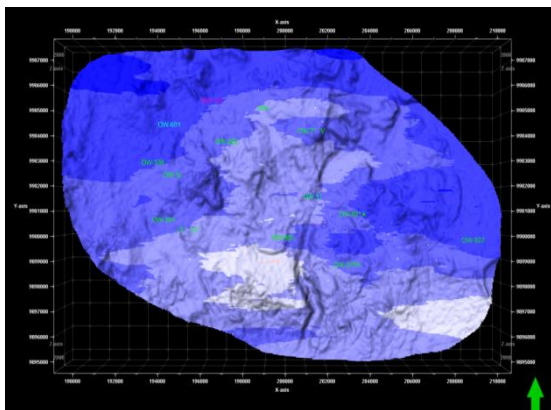


Figure 9: Iso-Resistivity map at 1900m.a.s.l

Resistivity map at 1900 m.a.s.l. presented in figure 9,10 and 11 show a resistivity of < 15 Ohm-m with the western side of the area covered by conductive formation of resistivity < 10 Ohm-m and the eastern side covered by fairly uniform resistivity of about 10  $\Omega$ m covering almost the entire area interpreted to be low temperature alteration minerals like smectite and zeolite formed as a result of hydrothermal alteration fluid filled fractures rock.

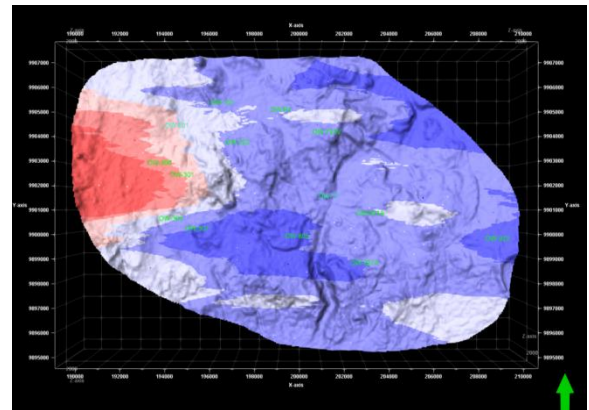


Figure 10: Iso-Resistivity map at 1900 m.a.s.l

Resistivity map at 1000 m.a.s.l. (Figure 12 and 13) about 1200m below the ground level shows moderately high resistivity (30 – 60 $\Omega$ m) to the eastern side of study area and persistent low resistivity of < 10 $\Omega$ m to the Western side (Oserian). The moderately high resistivity can be attributed to the presence of high temperature secondary minerals such as epidote, chlorite and biotite. The persistent conductive layer to the eastern side (Oserian) is interpreted to be due to the presence of low temperature alteration minerals like Smectite and Zeolite

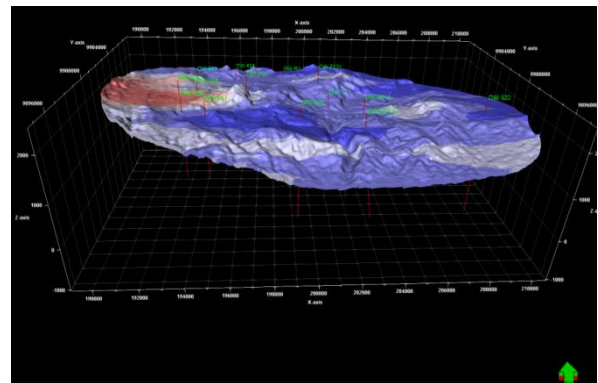


Figure 11: Iso-Resistivity map at 1900 m.a.s.l

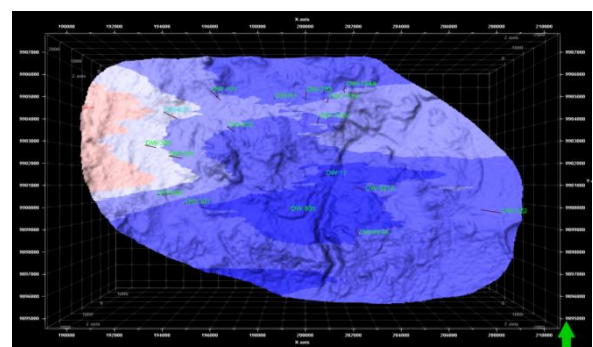


Figure 12: Iso-resistivity map at 1000 m.a.s.l.

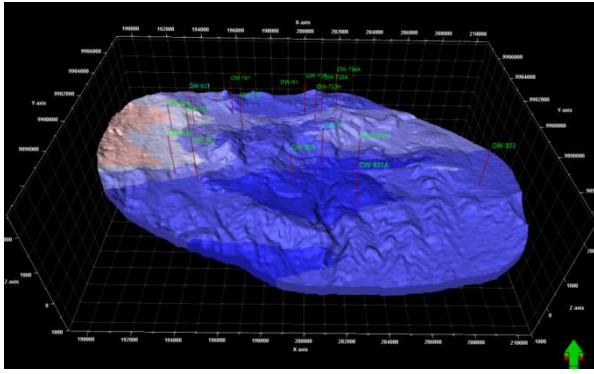


Figure 13: Iso-resistivity map at 1000 m.a.s.l.

Resistivity map at 500 M.a.s.l (Figure 14 and 15) about 2000 m below the ground level. The area is covered by medium to high resistivity (30 – 60Ωm). The high resistivity is seen to cover the central part extending to south and eastern side while the medium resistivity is seen to cover the western side (Oserian) of the study area. The high resistivity is interpreted to be due to the presence of high temperature alteration minerals while medium resistivity is attributed to the presence of low temperature alteration minerals. Findings from the data presented clearly define the resistive feature identified and marked at the center extending southwards may indicate the doming heat source also referred to as geothermal upwelling at shallow depth.

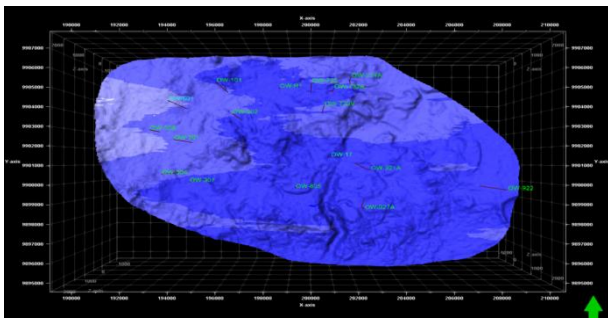


Figure 14: Iso-resistivity map at 500 m.a.s.l

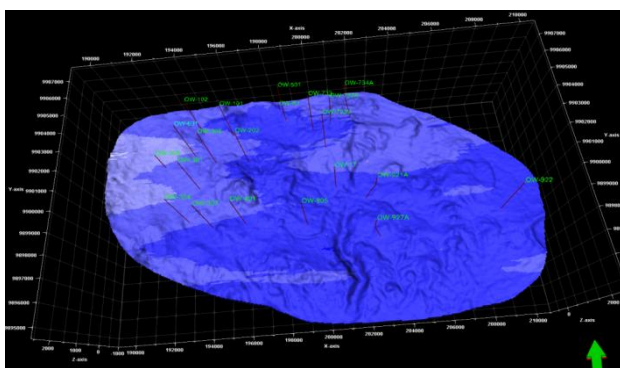


Figure 15: Iso-resistivity map at 500 m.a.s.l

Resistivity map at 0 m (Figure 16) about 2500 m below the ground level. The area is covered by medium to high resistivity (30 – 60Ωm). The high resistivity is seen to cover almost the entire area except eastern side. The high resistivity is interpreted to be due to the presence of high temperature alteration minerals while medium resistivity is attributed to the presence of low temperature alteration minerals. The increased geophysical survey to the east around OW-922 has revealed more information of the

presence of high temperature alteration which can be observed at 0 m.

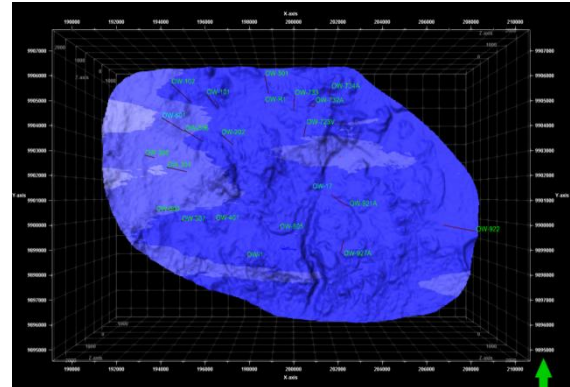


Figure 16: Iso-resistivity map at 0 m

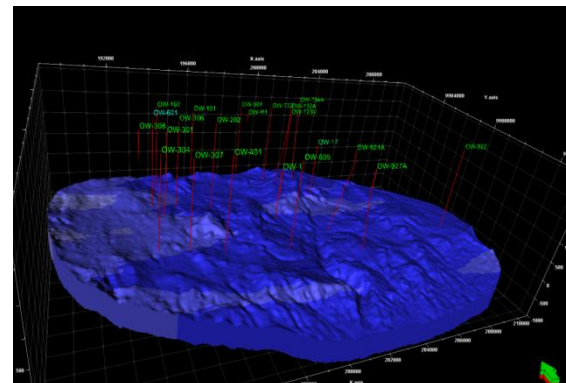


Figure 17: Iso-resistivity map at 200m.b.s.l

Resistivity map at 2000 M.b.s.l (Figure 4.14) about 4200 m below the ground level, high resistivity starts to diminish and low resistivity starts to spread. The appearing low resistivity anomaly is associated with the heat source which is structurally controlled.

## 8. Discussion of 1D Inversions

Resistivity structure in most high-temperature geothermal systems is characterized by a low resistivity cap at the outer margins of the reservoir, underlain by a more resistive core towards the inner part. This structure has been found in both freshwater systems as well as brine systems, with the later having lower resistivity's values. Comparison of this resistivity structure with data from wells has been carried in high temperature geothermal fields in Iceland and in the East African rift. The results have shown a good correlation with alteration mineralogy. This observation is of great importance, because the temperature dependence of the alteration mineralogy makes it possible to interpret the resistivity layering in terms of temperature, provided that the temperature is in equilibrium with the dominant alteration minerals.

Magnetotelluric (MT) method targets deep hot rocks that act as the heat source for a geothermal system under survey. From the results of the joint inversion of MT and TEM data of the Northwest Olkaria field a fairly good correlation with the available geological information is noted and the following resistivity structure can be deduced as seen on cross-sections and iso-resistivity maps. These areas can be



termed as potential reservoirs (Figure 18 and 19). The 1D joint inversion results (Figure 18 and Figure 19) of Olkaria geothermal complex reveal a resistivity structure with four layered resistivity zones. A shallow superficial high resistivity zone ( $> 30\Omega\text{m}$ ) thought to be due to unaltered rock formations and the thick pyroclastic cover is observed across the field. This is succeeded by a thick dome shaped conductive layer ( $< 6\Omega\text{m}$ ) that extends to about 200 m.a.s.l in the North West field and thins towards the Central field becoming almost uniform in the South East and the rest of the field. This layer is presumed to be dominated by low temperature alteration minerals such as smectite and zeolite and defines the clay cap. Beneath the base of this conductor is a resistive layer ( $>15\text{-}50\ \Omega\text{m}$ ) which is thought to be associated with the high temperature secondary minerals such as epidote, chlorite and biotite present in the reservoir.

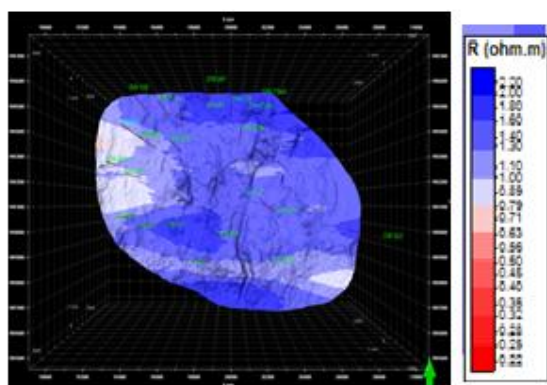


Figure 18: Iso-resistivity map at 2000 M.b.s.l

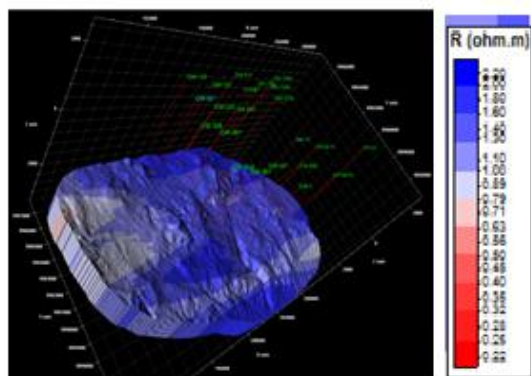


Figure 19: Iso-resistivity map at 2000 m.b.s.l

Underlying the resistive layer is another low conductivity layer extending to about 6,000 m.b.s.l(Figure 20) which could be associated with the heat source.

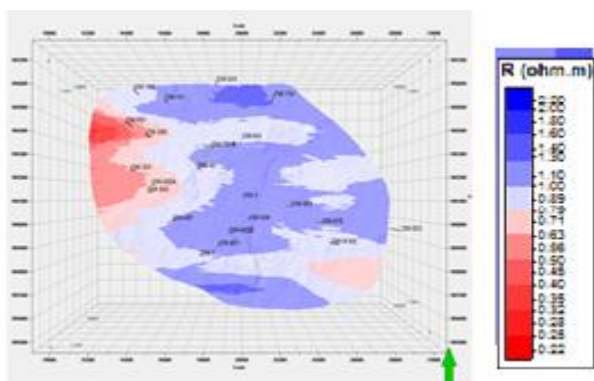


Figure 20: Iso-Resistivity maps at 6000 m.b.s.l

The deep wells in domes and Olkaria Central field correspond to the deep high resistivity anomaly defined by MT data, while the low productive wells fall within the generally conductive shallow subsurface layer. The shallow structure reflects the lithological response of shallow formations, which are quite conductive interpreted to due to the presence of low temperature alteration minerals. It is clear that the low resistivity cap on the western side is different with the low resistivity on the Eastern side. The western side is too conductive and thicker than the eastern side. Lack of alteration mineralogy of the drilled wells to the West (Oserian Wells) has made it difficult to correlate the alteration mineralogy with resistivity. The alteration mineralogy on the Eastern part of the study area is in agreement with resistivity.

Findings from the data presented clearly define the resistive feature identified and marked at the center extending southwards may indicate the doming heat source also referred to as geothermal upwelling at shallow depth expressed in the conceptual model presented in (Figure 21).

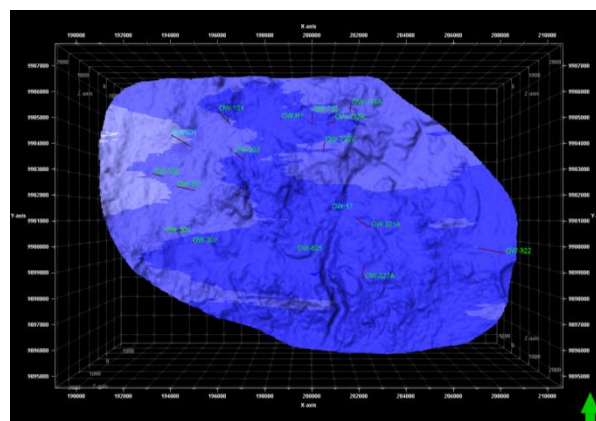


Figure 21: Conceptual model of NW field

The appearing low resistivity anomaly is associated with the heat source and geothermal reservoirs which are structurally controlled (figure 22).

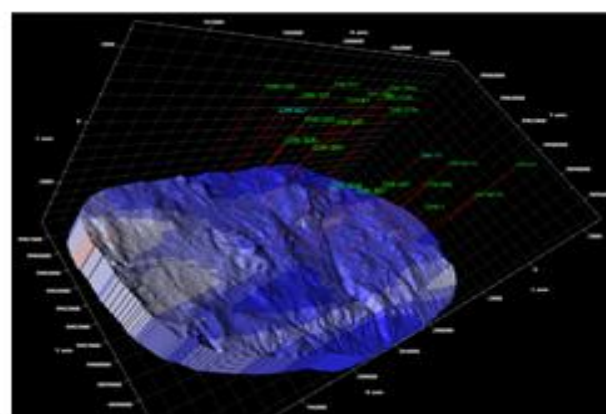


Figure 22: Positions of geothermal reservoirs in the NW field at 6000m.b.s.l.

Lithology based on well data shows that the shallow thin high resistivity layer corresponds to dry basaltic rocks covering the surface (Ofwona, 2008). The conductive layer reflects saline fluids but correlates also with low temperature alteration (smectite and zeolites), the deep resistive core



correlates with the high temperature alteration minerals (chlorite and epidote) whereas the deep seated conductive body is most likely connected to the heat source of the Olkaria geothermal system (Omenda, 2000).

## 9. Conclusions

In this project, modern MT exploration has been applied to structural imaging in the NW Olkaria prospect. The results have shown that with state-of-the-art of MT methodology, useful structural information can be obtained. Like any geophysical method, MT requires a contrast in material properties to image structures.

### 9.1 1D Joint Inversion of Magnetotelluric and Transient Electromagnetic Data

The 1D joint inversion results of Olkaria geothermal complex reveal a resistivity structure with four layered resistivity zones. A shallow superficial high resistivity zone thought to be due to the presence unaltered rock formations and thick dry pyroclastic cover is observed across the field. This is succeeded by a thick dome shaped conductive layer ( $< 6\Omega\text{m}$ ) that extends to about 700 m.a.s.l in the North West field and thins towards the Central field becoming almost uniform in the South East and the rest of the field. This layer is presumed to be dominated by low temperature alteration minerals such as smectite and zeolite and defines the clay cap. Beneath the base of this conductor is a resistive layer ( $>15\text{-}50\ \Omega\text{m}$ ) which is thought to be associated with the high temperature secondary minerals such as epidote, chlorite and biotite present in the reservoir. Underlying the resistive layer is another low conductivity layer extending to about 6,000 m.b.s.l which could be associated with the heat source.

### 9.2 1D Iso-resistivity Maps of Northwest Olkaria field

The iso-maps reveals the existence of a boundary at 500 m.a.s.l which is marked by wells OW-302, OW-306 and OW-401. The main reservoir to the western side appears to be deeper than the known situation in the eastern field. Lithology based on well data shows that the shallow thin high resistivity layer corresponds to dry pyroclasts covering the surface, the conductive layer reflects clays but correlates also with low temperature alteration (smectite and zeolites), the deep resistive core correlates with the high temperature alteration minerals (chlorite and epidote), at great depths, a prominent low resistive cap is observed and it is probably reflecting the presence of heat source of the geothermal system underneath the GOGA.

### 9.3 1D Magnetotelluric model of the Northwest Olkaria field

The resistivity cross-sections of joint 1D inversion of MT and TEM data show a geothermal system with four major resistivity zones delineated. These inversions were achieved by fitting both data kinds using the same 1D resistivity model. The result of the interpretation shows four main resistivity structures below the geothermal area: A shallow superficial lying thin high resistivity layer ( $> 30\Omega\text{m}$ ) thought to be due to unaltered rock formations and the thick pyroclastic cover is observed across the field followed by

low resistivity thick dome shaped conductive layer ( $< 6\Omega\text{m}$ ) that extends to about 200 m.a.s.l in the North West field and thins towards the Central field becoming almost uniform in the South East and the rest of the field. This layer is presumed to be dominated by low temperature alteration minerals such as smectite and zeolite and defines the clay cap. Below there is a high resistivity layer (resistive core) underlain by a deep lying conductor ( $>15\text{-}50\ \Omega\text{m}$ ) which is thought to be associated with the high temperature secondary minerals such as epidote, chlorite and biotite present in the reservoir. Underlying the resistive layer is another low conductivity layer extending to about 6,000 m.b.s.l. which could be associated with the heat source. Lithology based on well data shows that the shallow thin high resistivity layer corresponds to dry basaltic rocks covering the surface, the conductive layer reflects saline fluids but correlates also with low temperature alteration (smectite and zeolites), the deep resistive core correlates with the high temperature alteration minerals (chlorite and epidote) whereas the deep seated conductive body is most likely connected to the heat source of the Olkaria geothermal system.

## 10. Recommendations

From the results discussed in this report, there are indications that the resource extends beyond OW-922 and we recommend for further exploration drilling east of OW-922. Exploration results from North West indicate resource boundary to be around OW-101 and therefore further drilling can be well guided by Figure 22. However we also recommend for exploration drilling west of OW-601 and OW-301 to be able to understand the cause of the low resistivity anomaly covering that area.

Geothermal exploration and development doesn't rely on results provided by a single method; it is recommended that 3D interpretation of the same data points to be done and used to constrain the results from 1D modeling and other exploration methods for better understanding of GOGA geothermal system. Further infill measurements are encouraged for the future geothermal resource development in GOGA field. Seismic monitoring is recommended for monitoring of the production field. The conceptual model should be reviewed and reconstructed with the latest gravity, magnetic and seismic results for better estimation of geothermal reservoir in GOGA.

In terms of future work, the following tasks should be the focus of future research:

- 1) To investigate three dimensional structures, it would be useful to make a new MT profile about 10-20 km away and parallel to this profile. The two surveys could constrain along strike changes of the resistivity structure.
- 2) The large spacing between some MT stations on the profile might give some artifacts in the inversion. Although the key features on the inversion model have been tested by modeling and inversion studies, these gaps may be significant. Some new measurements should be made in these gaps in future.
- 3) We recommend that more long period MT and TEM data (at the same location) be acquired and 3D data interpretation be carried out to define three-dimensional

features in the area. An integrated approach of data interpretation should also be adopted to incorporate all geophysical data. To understand the depth to the heat source and structures of the area, seismic studies both active and passive should be carried out in the area.

## 11. Acknowledgments

I would like to express my sincere appreciation to the Geophysics department of The Kenya Electricity Generating Company (KenGen) for their indispensable support; technical guidance, advice and helpful comments from the beginning to the end of this research. This project would not have been completed without your constant supervision of my supervisors Elvis Oduong, Ammon Omiti and Martin Owiso from Kenya electricity generating company.

## References

- [1] Abdelfettah, Y., Tiercelin, J. J., Tarits, P., Hautot, S., Maia, M., & Thuo, P. (2016). Subsurface structure and stratigraphy of the northwest end of the Turkana Basin, Northern Kenya Rift, as revealed by magnetotellurics and gravity joint inversion. *Journal of African Earth Sciences*, 119, 120-138.
- [2] Árnason, K., (2006). TEMTD, a programme for 1-D inversion of central-loop TEM and MT data. Short manual. *Iceland GeoSurvey - ISOR*, internal report, 17 pp.
- [3] Árnason, K., 1989: Central-loop transient electromagnetic sounding over a horizontally layered earth. *Orkustofnun, Reykjavík, report OS-89032/JHD*, 6, 129 pp.
- [4] Boashash, B. (2015), Time-frequency signal analysis and processing: a comprehensive reference. *Academic Press* 65,23-45.
- [5] Christiansen, A.V., Auken, E. and Sørensen, K. (2006). The transient electromagnetic method. *Groundwater geophysics*, 56, 642-647
- [6] Eysteinnsson, H., (1998), TEMMAP and TEMCROSS plotting programs. *Iceland GeoSurvey - ÍSOR*, Unpublished programs and manuals, 23, 28-54
- [7] Jones, A.G., (1988), Static shift of magnetotelluric data and its removal in a sedimentary basin environment. *Geophysics*, 53(7), 967-978
- [8] Khazri, D., & Gabtni, H. (2018), Geophysical methods integration for deep aquifer reservoir characterization and modeling (SidiBouzid basin, central Tunisia). *Journal of African Earth Sciences*, 138, 289-308
- [9] Odera, P. A. (2016). Assessment of EGM2008 using GPS/levelling and free-air gravity anomalies over Nairobi County and its environs. *South African Journal of Geomatics*, 5 (1), 17-30.
- [10] Ofwona, C., (2008), Geothermal Resource Assessment- Case Example Olkaria 1, Presented at Short Course III on Exploration for Geothermal Resources, *UNU- GTP*, 3, 18-19
- [11] Oldenburg, D.W., 1979, One dimensional inversion of natural source Magnetotelluric observations, *Geophysics*, 44, 1218-1244
- [12] Omenda, P., (2000), Anatectic origin for Comendite in Olkaria geothermal field, Kenya Rift; Geochemical evidence for syenitic protholith. *African Journal of Sciences and Technology. Science and Engineering series*, 1(68), 39-47
- [13] Omenda, P., and Simiyu, S. (2015). Country update report for Kenya 2010–2014. *Proceedings World Geothermal*, 34, 60-72
- [14] Ouma, P.A., (2010), Geothermal exploration and development of the Olkaria geothermal field. Paper presented at *Short Course V on Exploration for Geothermal Resources organized by UNU-GTP, GDC and KenGen, at Lake Bogoria and Lake Naivasha, Kenya*, 5, 16pp
- [15] Pellerin, L., and Hohmann, G.W., (1990), Transient electromagnetic inversion: A remedy for magnetotelluric static shifts, *Geophysics*, 55, (9), 1242-1250
- [16] Prodehl, C., Ritter, J., Mechie, J., Keller, G.R., Khan, M.A., Fuchs, K., Nyambok, I.O., Obel, J.D., (1997), The KRISP 94 Lithospheric investigation of southern Kenya-the experiments and their main results, In: Stress and stress release in the Lithosphere, *Tectonophysics*, 278, 121-148
- [17] Renaut, R. W., Owen, R. B., & Ego, J. K. (2017). Geothermal activity and hydrothermal mineral deposits at southern Lake Bogoria, Kenya Rift Valley: Impact of lake level changes. *Journal of African Earth Sciences*, 129, 623-646
- [18] Sternberg, B. K., Wash Bourne, J.C., Pullerin, L., (1988), Correction for the static shift in Magnetotellurics using Transient Electromagnetic soundings. *Geophysics*, 53, 1459-1468
- [19] Telford, W. M., Geldart, L. P., & Sheriff, R. E. (1990). *Applied geophysics*, Cambridge university press, 1, 110-117
- [20] Wadge, G., Biggs, J., Lloyd, R., & Kendall, J. M. (2016). Historical volcanism and the state of stress in the East African Rift System. *Frontiers in Earth Science*, 4, 86pg
- [21] Wamalwa, A. M., Kevin, L.M. and Laura, F.S., (2013), Geophysical characterization of the Menengai volcano, central Kenya Rift from the analysis of the magnetotelluric and gravity data, *geophysics*, 78(4), 187-199
- [22] Ward, S.H., and Wannamaker, P.E., (1983), the MT/AMT electromagnetic method in geothermal exploration, *UNU-GTP, Iceland, report 5*, 107 pp
- [23] West-JEC, (2006), The Olkaria Optimization Study – Phase I final report. *West Japan Engineering Consultants, Inc.* 1, 52-59